Surface Rheology of Monolayers of Poly(1-alkylene-*co*-maleic acid) at the Air/Water Interface: Surface Light Scattering Studies

Chanjoong Kim,[‡] Alan R. Esker,[§] Frank E. Runge,[⊥] and Hyuk Yu*,[†]

Department of Chemistry, University of Wisconsin−Madison, Madison, Wisconsin 53706; Division of Engineering and Applied Sciences, Harvard University, Cambridge, Massachusetts 02138; Department of Chemistry, Virginia Polytechnic Institute and State University, Blacksburg, Virginia 24061; and Agricultural Products, BASF Aktiengesellschaft, D-67117 Limburgerhof, Germany

Received March 2, 2006; Revised Manuscript Received May 2, 2006

ABSTRACT: The surface viscoelasticity of poly(1-alkylene-*co*-maleic acid) (PXcMA) with side chains varying from C4 to C16 was investigated at the air/water interface using the technique of surface light scattering (SLS). In the dilute surface mass density regime, the side chain length of the 1-alkylene has been shown to produce a wide range of surface viscoelastic films, from an elasticity-dominant film to a viscosity-dominant film. On the other hand, in the semidilute surface mass density regime, the film viscoelasticity is scarcely affected by the side chain length. Rather, the viscoelastic parameters are shown to scale with the inverse of surface mass density, i.e., area per monomer *A*. An inference is drawn that interactions between the hydrophilic polymer head of maleic acid moiety and the interface dominate in this regime. The loss tangent value varies with the side chain length in the dilute regime, whereas it no longer depends on the side chain length in the semidilute regime, where it collapses onto a limiting scaling behavior hitherto unknown: $\tan \delta \sim A^{-10} \sim \Pi^2$.

Introduction

The monomolecular layer is a primordial interfacial object. Hence, the interest in monolayers necessarily attends the current feverish activities in science and technology of interfaces. In particular, a significant fraction of the constituents of thin films and nanoparticles may be found at the interface relative to those in bulk. Monolayers at gas/liquid and liquid/liquid interfaces have been attracting recent interest since the resurgence of Langmuir−Blodgett films for the past three decades. Thus, there has accumulated a sizable literature[1−3] that deals with amphiphilic molecules of various kinds, collectively called surfactants. They form not only planar monolayer films at the air/water interface (A/W) but also micelles of various shapes, vesicles, emulsions, foams, and bilayers. The main characteristics of common surfactants are intramolecular segregation of the hydrophilic and hydrophobic moieties. Polymeric surfactants, on the other hand, differ from this molecular architecture. There are two main categories, i.e., vinyl polymers with pendant hydrophilic groups and block copolymers with hydrophobic and hydrophilic blocks. The former is often referred to as a chain with "a greasy backbone decorated with wet feet". Polymeric surfactants are of special interest in terms of their interfacial dynamics by virtue of their conformational changes arising from molecular size and/or chain connectivity.

Rheology of surfactant monolayers is critical in film formation and dynamic stability of gas/liquid and liquid/liquid interfaces. Particularly, it impacts on designs of full and complete transfer of monolayers in Langmuir−Blodgett films. In complete parallel with polymeric systems in bulk or concentrated solution, materials design of polymeric surfactants crucially hinges on their interfacial rheology. Thus, we focus our attention on a particular system of polymeric surfactants, an alternating copolymer of 1-alkylene and maleic anhydride that is subsequently hydrolyzed. Commercial applications of this system have been explored as coating, emulsifying, and foaming agents by several industrial firms.[4]

Since the advent of a noninvasive optical technique called surface light scattering (SLS), the static and dynamic behavior of a fair number of polymeric and small molecule surfactant monolayers have been examined. Earlier investigations for insoluble monolayers at the air/water interface were performed by Hård and Neuman,[5] Langevin,[6] and this group.[7−9] The SLS technique probes the propagation characteristics of spontaneously formed capillary waves, normally in conjunction with the Wilhelmy plate technique for simultaneous monitoring of the static surface tension. Surface pressure isotherms ($\Pi-A$) are used to deduce the reversible compressive (and dilational) modulus of monolayers, where the surface pressure Π is defined as the surface tension difference between pure and film-covered interfaces which is a function of surface mass density (Γ) or its inverse, area per repeating unit of polymer (A). For short, the repeating unit is referred to as "monomer". The SLS technique has been used to extract two-dimensional dynamic elasticity, ϵ_d, and the corresponding viscosity, κ. A canonical example of vinyl polymer surfactants, namely poly(vinyl acetate), at the air/water interface was first systematically examined by SLS,[10] and subsequently other systems were investigated to gain further insight into the interfacial dynamics.[11−15]

We now explain briefly the scaling behavior of polymer monolayers. When Π is greater than 1 mN m^{-1}, a power law relationship exists for Π and A. The basis for the scaling laws in 2D and 3D is well established theoretically and computationally.[16,17] One well-known scaling relationship is $R_G \sim N^{\nu}$, where R_G is the radius of gyration of the polymer chain, N is the number of repeating units of the chain, and ν is the static scaling exponent. The scaling relationship that describes the dependence of Π on Γ or A for a polymer monolayer at the A/W interface is

$$\Pi \sim \Gamma^{z} \sim A^{-z} \quad (1)$$

[†] University of Wisconsin−Madison.
[‡] Harvard University.
[§] Virginia Polytechnic Institute and State University.
[⊥] BASF Aktiengesellschaft.

10.1021/ma0604643 CCC: $33.50
Published on Web 06/13/2006

where z is the scaling exponent, related to the static scaling exponent ν such that $z = 2\nu/(2\nu - 1)$ in the semidilute regime while $z = 1$ in the dilute regime.[18] Based on 2D considerations, the predicted upper limit of z is 101 ($\nu = 0.505$)[19] for the theta condition and the lower limit is 2.86 ($\nu = 0.769$)[20] for the good solvent condition.

Turning to the surface light scattering experiment, we start with the fact that the presence of a monolayer at the A/W interface reduces the surface tension and affects the damping of surface motions. Changes in the propagation characteristics of spontaneously formed capillary waves can be deduced from the method of surface light scattering (SLS) combined with the Wilhelmy plate technique[21] to simultaneously detect changes in surface tension. Hydrodynamic models developed to describe the motion of the monolayer-covered surface are then used to extract viscoelastic parameters from the SLS power spectrum. We adopt the Lucassen−Lucassen−Reynders dispersion relation:[22]

$$\eta^2(k - m^*)^2 = \left[\eta(k + m^*) + \frac{\epsilon^* k^2}{i\omega^*}\right]\left[\eta(k + m^*) + \frac{\sigma^* k^2}{i\omega^*} + \frac{g\rho}{i\omega^*} - \frac{\omega^*\rho}{ik}\right] \quad (2)$$

$$m^* = \left(k^2 + \frac{i\omega^*\rho}{\eta}\right)^{1/2}, \quad \mathrm{Re}\,(m^*) > 0 \quad (3)$$

$$\omega^* = \omega_0 + i\alpha \quad (4)$$

$$\omega_0 = 2\pi f_s \quad (5)$$

$$\alpha = \pi\Delta f_{s,c} \quad (6)$$

$$\sigma^* = \sigma_d + i\omega^*\mu \quad (7)$$

$$\epsilon^* = \epsilon_d + i\omega^*\kappa \quad (8)$$

where k is the spatial wave vector, ϵ_d is the dynamic longitudinal elasticity, κ is the corresponding viscosity (that is, the sum of the dilational and shear components in the monolayer), η and ρ are the bulk steady shear viscosity and density of the subphase, σ_d is the dynamic surface tension, and μ is the transverse viscosity of monolayer. The frequency shift (f_s) and the instrument width corrected spectral width ($\Delta f_{s,c}$) are experimentally determined from SLS by fitting the observed power spectrum with the Lorentzian profile. Using these experimental parameters, ϵ_d and κ can be calculated from the dispersion equation, if the following assumptions are made: (1) σ_d is the same as the static surface tension (σ_s) determined by the Wilhelmy plate method, (2) μ is negligibly small, and (3) ϵ_d and κ are independent of the wave vectors within our accessible range. These assumptions were tested and found to be plausibly justified.[6,12,23,24] Not so parenthetically, we should note that an alternative scheme to extract all four parameters σ_d, μ, ϵ_d, and κ exists by analyzing the full time-domain signal of scattered light. This approach was advocated by Earnshaw and coworkers[25] and implemented by Richards' group[11] for the viscoelastic characterization of syndiotactic poly(methyl methacrylate) monolayers on A/W. We choose the simpler scheme in view of our limited range of accessible spatial wave vector k. Further, it is our observation that quantitative specification of σ_d and μ does not add much more[26] to the dynamic characterization than $\sigma_d \approx \sigma_s$ and $\mu \approx 0$.

A reference interface is useful to compare monolayer dynamics. Specified values of σ_d, μ, ρ, and η for water at 25 °C and a given scattering wave vector, k, are used to compute the propagation parameters of capillary waves ($\Delta f_{s,c:eq}$, the damping coefficient, and $f_{s:eq}$, the propagation frequency, where the subscript eq stands for equivalent) for different values of ϵ_d and κ.[9] Once the reference interface is specified, all monolayers with known ϵ_d and κ can be compared by computing the corresponding capillary wave propagation parameters. Alternatively, the loss tangent (tan δ) can be used to analyze the surface viscoelasticity. The loss tangent is the ratio of viscous dissipation energy to elastic storing energy, defined as the ratio of the loss modulus to the storage modulus

$$\tan\delta = \kappa\omega_0/\epsilon_d \quad (9)$$

Hence, when tan δ is less than the unity, the film elasticity is said to be dominant. Conversely, if tan δ is larger than the unity 1, the film viscosity is said to be dominant.

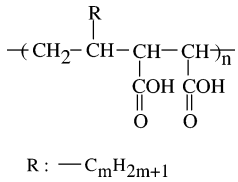

Figure 1. Structure of the hydrolyzed form of PXcMA polymer where X = H (hexylene) for $m = 4$, O (octylene) for $m = 6$, D (decylene) for $m = 8$, and OD (octadecylene) for $m = 16$, for each α-olefin uses two carbons in the chain backbone.

Table 1. Molecular Weights of Poly(1-alkylene-*co*-maleic acid) (PXcMA)

sample	M_w/kg mol^{-1}	M_w/M_n
PHcMA	34	4.2
POcMA	18	2.6
PDcMA	30	3.4
PODcMA	128	2.9

Earlier, we have shown that the surface viscoelasticity at the A/W interface is strongly dependent on the hydrophilicity of the polymer[9] and on the side-chain length and packing.[13] In a previous report, we made a binary comparison relative to the role of chain length and side-chain packing using poly(vinyl acetate) (PVAc) and poly(octadecylene-*co*-maleic acid) (PODcMA). This report is prompted by that comparison. Here, we examine a more systematic approach with express purposes of probing the interfacial dynamics on A/W with a system of amphiphilic polymers, poly(1-alkylene-*co*-maleic acid), by holding the same hydrophilic headgroup while varying the length of hydrophobic side chain, from C4 to C16. The polymer system is designated as PXcMA, where X varies from 1-hexylene to 1-octadecylene.

Experiment Section

Materials and Monolayer Preparation. Dr. Calvin J. Verbrugge of Johnson Polymer of Sturtevant, WI, provided a series of PXcMA polymers: hexylene, octylene, decylene, and octadecylene, corresponding to X = H, O, D, and OD, respectively (Figure 1). These polymers were polymerized as alternating copolymers of 1-alkylene and maleic anhydride. We have subsequently hydrolyzed and purified in accord with the procedure outlined elsewhere.[13] Some of the samples were provided to us by Dr. Julia S. Tan of Kodak after very careful purification. Table 1 lists the results of the GPC analysis performed by Dr. Thomas H. Mourey of Eastman Kodak. Spreading solutions with concentrations of 0.01−0.03 g/L were prepared in a mixed solvent of hexane and THF (3:1). To prevent ionization of the polymers, the subphase was maintained at pH 2 with 0.01 M HCl (Aldrich, 99.999%).

Surface Pressure and Static Surface Elasticity. A Langmuir trough made of Teflon and chamber have been described in detail

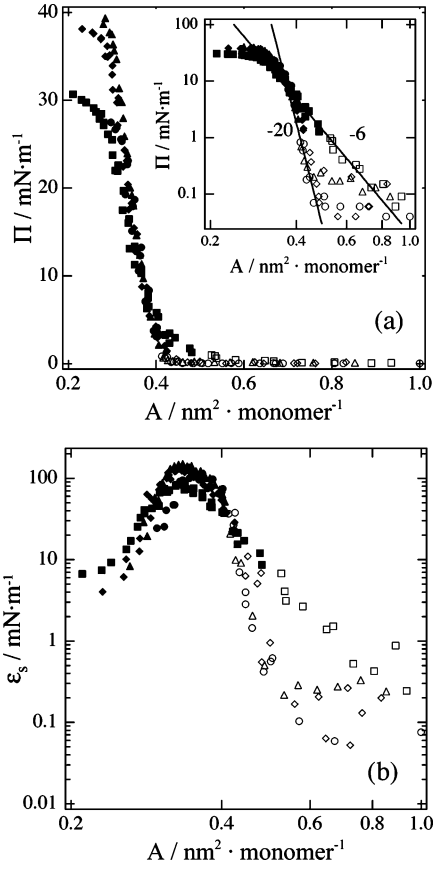

Figure 2. (a) Π−*A* isotherms and (b) ϵ_s−*A* for PXcMA polymers on 0.01 M HCl at 25 °C, both in a double-logarithmic plot. Squares are for PHcMA, diamonds for POcMA, triangles for PDcMA, and circles for PODcMA. Open symbols are used for the dilute regime (Π ≤ 1 mN m^{-1}) and filled symbols for the semidilute regime (Π > 1 mN m^{-1}).

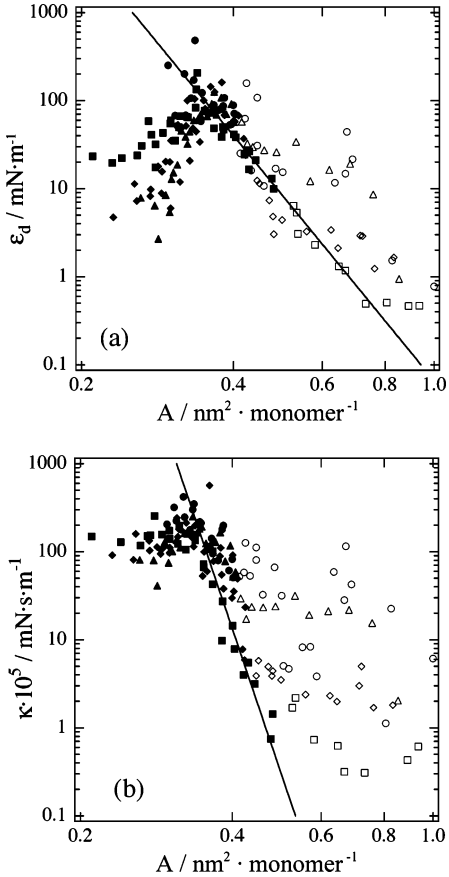

Figure 3. (a) ϵ_d−*A* and (b) κ−*A* for PXcMA polymers on 0.01 M HCl at 25 °C. The symbols are the same as Figure 2. The solid line is drawn over the data for PHcMA. The values represent an average over three wave vectors and error bars are omitted for clarity, but they amount to about 10% and 15% respectively for ϵ_d and κ.

previously.[27] The successive addition method was used to vary the surface mass density of polymer on the surface. The static surface tension (σ_s) was measured with a Cahn 2000 electrobalance. The equilibrium surface tension was determined after the time dependence of surface, dσ_s/dt, decays to less than about 10^{-3} mN/(m min).

Assuming that the entire mass of the spread polymer remains on the surface without any desorption into the subphase, A, in units of nm^2/monomer, was calculated and plotted against Π (Figure 2). The static elasticity, ϵ_s, was obtained from the surface pressure−surface area per monomer (Π−*A*) isotherm by

$$\epsilon_s = -A\left(\frac{\partial \Pi}{\partial A}\right)_T \tag{10}$$

which is the surface analogue of the bulk modulus, $B \equiv -v(\partial P/\partial v)_T$, where P is the isotropic pressure and v is the volume.

Surface Light Scattering. The SLS experimental setup has been described in detail elsewhere.[21] Here, we explain some recent modifications. The scattered light from a He−Ne laser (7 mW, 632.8 nm, Melles Griot 05LHP 171) incident at an angle of 64.3° normal to the surface is selected with a transmission diffraction grating to provide a reproducible source for the heterodyne beating. The signal was sent to a PC for fast Fourier transform (FFT) and averaging for 512 counts. In this work the fourth-, fifth-, and sixth-order diffraction spots were used to define the scattering angle, with the corresponding wave vectors of k = 266, 328, and 389 cm^{-1}, respectively.[27] For each surface density, the power spectra of these three wave vectors were obtained and the viscoelastic properties (ϵ_d, κ, $\Delta f_{s,c:eq}$, $f_{s:eq}$, and tan δ) were calculated individually. We show only averaged values of these dynamic properties from the three wave vectors without error bars for clarity.

Results and Discussion

With the exception of PHcMA, the Π−*A* isotherms of the polymer monolayers (Figure 2a) are nearly identical, and they are consistent with the expected isotherms of condensed films. The isotherms are shown in two regions: the dilute regime where Π ≤ 1 mN m^{-1} (open symbols) and the semidilute regime where Π > 1 mN m^{-1} (filled symbols); the reason for this will become clear. The critical scaling exponent z in eq 1 for PHcMA is 6, while z for the others is about 20. This suggests that the A/W interface is a poor solvent for PXcMA polymers, but a slightly better solvent for PHcMA.[28] The static elasticity ϵ_s values (Figure 2b) for PXcMA polymers are distinguishable in the dilute regime but collapsed together in the semidilute regime, again with the exception of PHcMA. The critical area A^* when the elasticity reaches a maximum, is 0.33−0.35 nm^2 for all PXcMA polymers and calculated $\epsilon_{s,max}$ value via eq 10 ranges from 80 to 140 mN m^{-1}. All values of A^* for PXcMA are smaller than twice A^* of 0.18 nm^2 for PVAc, a prototype surface active vinyl polymer, whereas $\epsilon_{s,max}$ is higher than those of the vinyl polymers.[8] The basis of this comparison arises from the fact that PXcMA backbone repeating unit (monomer) has four carbons while that of vinyl polymers have two carbons. This difference suggests that PXcMA polymers pack more efficiently than the vinyl polymers.

The dynamic viscoelastic parameters, ϵ_d and κ, are displayed in Figure 3. In general, both parameters parallel the behavior of ϵ_s, increasing with lateral packing (decreasing A) up to A^* ≈ 0.32 nm^2/monomer and then decreasing. In the dilute regime (open symbols), longer side chain polymers produce only

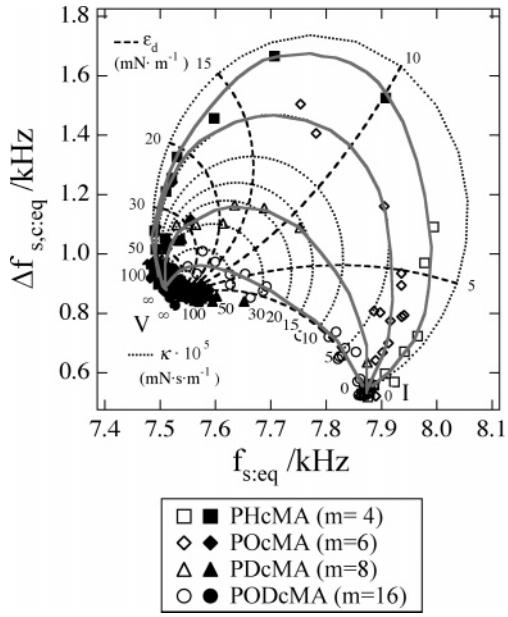

Figure 4. Polar plot for PXcMA polymers on 0.01 M HCl at 25 °C. The symbols are the same as Figure 2. Solid curves are drawn through the points to indicate the overall trends. $\Delta f_{s,c:eq}$ and $f_{s:eq}$ are calculated on the basis of the reference state that $k_{ref} = 324.3$ cm^{-1}, $\eta_{ref} = 0.894$ cP, $\rho_{ref} = 0.997$ g/cm^3, $\sigma_{d,ref} = 71.79$ mN/m, and $\mu_{ref} = 0$ mN·s/m (water at 25 °C). The solid curves correspond to constant value of ϵ_d while the dashed loops correspond to constant $\kappa \times 10^5$ value. The values are averages over three wave vectors, and error bars (amounting to about 20%) are omitted for clarity.

slightly higher ϵ_d values than those with shorter side chains. On the other hand, κ shows a clear side-chain dependence; the longer the side chain, the higher the value of κ. In the semidilute regime (filled symbols), however, all of the polymers appear to be the same.

In Figure 4 are displayed a reference polar plot; that is, the equivalent spectral width $\Delta f_{s,c:eq}$ is plotted against the corresponding spectral shift $f_{s:eq}$ of all four PXcMA polymers. PHcMA (C4 side chain) follows the profile of an almost purely elastic surface film, whereas chains with longer side chains follow that of progressively more viscous profiles of the films. The deviation from a purely elastic film increases with increasing side chain length, and it is shown to be most pronounced for PODcMA (C16). Some insights into the monolayer viscoelasticity with respect to the polymer structures are gained from such a polar plot but are seemingly limited to the dilute regime. Once the surface mass density is increased to the semidilute regime, the data are all crowded around region V, obscuring their viscoelastic behaviors. Plotting the ratio of the loss modulus to the storage modulus, i.e., tan δ, against A and Π (Figure 5) provides a better comparison. In the dilute regime, tan δ of each polymer is distinguishable and monotonically decreasing with decreasing A. A polymer with longer side chains has a higher tan δ value (is more viscous) than one with shorter side chains, although the values are somewhat scattered for PODcMA. Presumably, the longer side chains interact more dissipatively with the A/W interface. In the semidilute regime, decreasing A increases tan δ for all PXcMA polymers, producing a limiting scaling behavior of tan $\delta \sim A^{-10} \sim \Pi^2$ regardless of the side-chain length. Thus, tan δ shows a clearer scaling with A than with Π for high surface concentrations. In other words, tan δ in the semidilute regime is more closely related to the surface mass density of monomers at the interface than to the surface pressure, which is related to not only the mass density of monomers but also the length of side chains.

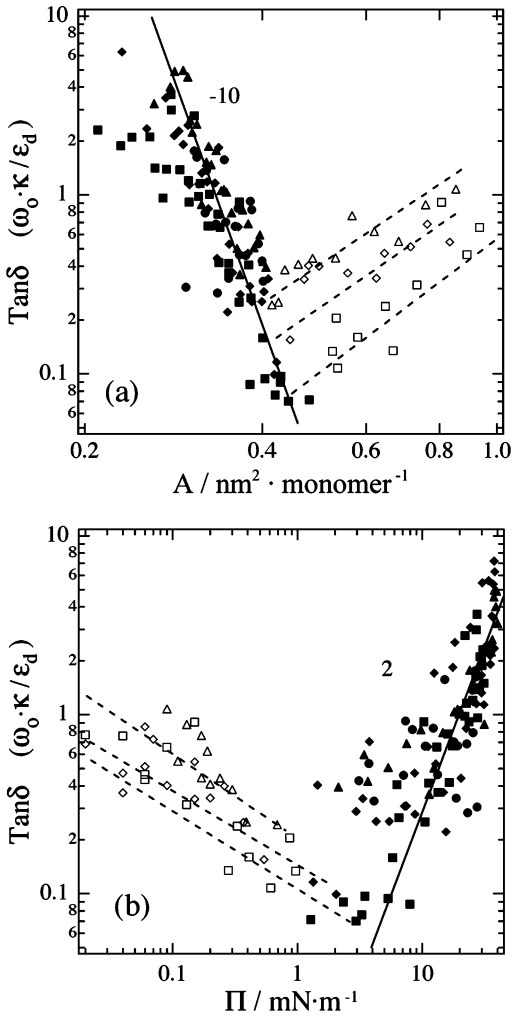

Figure 5. Loss tangent (tan δ) for PXcMA polymers on 0.01 M HCl at 25 °C. The symbols are the same as Figure 2. The dashed lines are guidelines for each polymer, and the solid line shows the slope of tan δ at high Π or at small A; tan $\delta \sim A^{-10} \sim \Pi^2$. The values represent averages over three wave vectors with error bars amounting to about 30% omitted for clarity. In both plots, PHcMA data in the dilute regime are not included since they are scattered much more than the rest, whereas the conclusion drawn for the semidilute regime is not affected by the omission.

Here, we propose an explanation. In the dilute regime, side chains lie down or thermally fluctuate and interact with the interface (Figure 6a). With increasing lateral packing or decreasing A, the side chains start to leave the interface and the viscous contribution to tan δ decreases. In the semidilute regime the side chains are standing up in the air, and only the backbone can interact with the air/water interface (Figure 6b).

Conclusions

The results of our study suggest that the main mechanism of viscous dissipation of this series of PXcMA polymers at the A/W interface occurs by interactions between the polymer chains and the interface rather than by interactions between the polymer chains. In the dilute regime, the surface viscoelasticity of the monolayers can be tuned by changing the side chain length of the α-olefin. However, in the semidilute regime the surface viscoelasticity is mainly dependent on the surface mass number density, not on the side chain length, and the loss tangent shows a limiting scaling: tan $\delta \sim A^{-10} \sim \Pi^2$. This distinctive difference in viscoelasticity may be related to the side-chain orientation. At low concentrations, the side chains lie on the

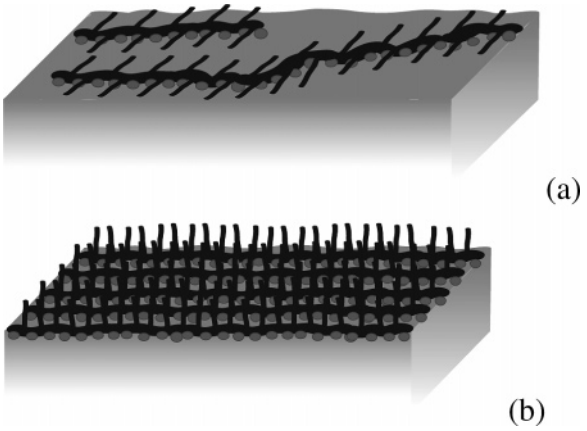

Figure 6. Cartoons describing PXcMA polymer monolayers at A/W (a) in the dilute regime and (b) in the semidilute regime. Gray balls represent hydrophilic carboxyl groups, and black lines represent hydrocarbon chains.

surface and dissipate energy through interactions with the interface, so a polymer with longer side chains dissipates more energy than one with shorter side chains. The increasing surface concentration in the semidilute regime causes the side chains to stand up, so energy dissipation occurs mainly through the interaction between the interface and the polymer backbone chain, which is much less hydrophobic than the side chain.

Acknowledgment. We are deeply indebted to Dr. Calvin J. Verbrugge of Johnson Polymer and Dr. Julia S. Tan of Kodak for their generous gift of the samples and Dr. Thomas H. Mourey of Kodak for his assistance in the sample characterization. This was in part supported by an NSF Grant (DMR-0084301) and by the professorship awarded to H.Y. by the Eastman Kodak Company.

References and Notes

(1) Adamson, A. W.; Gast, A. *Physical Chemistry of Surfaces*, 6th ed.; Wiley: New York, 1995; Chapter IV.
(2) Butt, H.-J.; Graf, K.; Kappl, M. *Physics and Chemistry of Interfaces*; Wiley-VCH: Weinheim, 2003; Chapters 12 and 13.
(3) deGennes, P.-G.; Brochard-Wyart, F.; Quere, D. *Capillarity and Wetting Phenomena*; Springer: New York, 2004; Chapter 8.
(4) For the commercial uses of these polymers, Kuraray of Japan commercializes one product under a name of ISOBAM, Johnson Polymer of Sturtevant, WI, with a set of the polymers under a name of JONOMA (US patents 4358573, 4522992, 4871823, 6020061) and Eastman Kodak (US patent pending) as emulsifying agents for photographic uses.
(5) Hård, S.; Neuman, R. D. *J. Colloid Interface Sci.* **1981**, *83*, 315.
(6) Langevin, D. *J. Colloid Interface Sci.* **1981**, *80*, 412.
(7) Kawaguchi, M.; Sano, M.; Chen, Y. L.; Zografi, G.; Yu, H. *Macromolecules* **1986**, *19*, 2606.
(8) Sauer, B. B.; Kawaguchi, M.; Yu, H. *Macromolecules* **1987**, *20*, 2732.
(9) Esker, A. R.; Zhang, L. H.; Sauer, B. B.; Lee, W.; Yu, H. *Colloids Surf., A* **2000**, *171*, 131.
(10) Kawaguchi, M.; Sauer, B. B.; Yu, H. *Macromolecules* **1989**, *22*, 1735.
(11) Henderson, J. A.; Richards, R. W.; Penfold, J.; Thomas, R. K. *Macromolecules* **1993**, *26*, 65.
(12) Yoo, K. H.; Yu, H. *Macromolecules* **1989**, *22*, 4019.
(13) Lee, W. K.; Esker, A. R.; Yu, H. *Colloids Surf., A* **1995**, *102*, 191.
(14) Esker, A. R.; Zhang, L. H.; Olsen, C. E.; No, K.; Yu, H. *Langmuir* **1999**, *15*, 1716.
(15) Zhang, L. H.; Esker, A. R.; No, K.; Yu, H. *Langmuir* **1999**, *15*, 1725.
(16) Doi, M.; Edward, S. F. *The Theory of Polymer Dynamics*; Oxford University Press: New York, 1986.
(17) Rubinstein, M.; Colby, R. H. *Polymer Physics*; Oxford University Press: New York, 2003.
(18) Daoud, M.; Cotton, J. P.; Farnoux, B.; Jannink, G.; Sarma, G.; Benoit, H.; Duplessix, R.; Picot, C.; de Gennes, P. G. *Macromolecules* **1975**, *8*, 804.
(19) Stephen, M. J.; McCauley, J. L. *Phys. Lett. A* **1973**, *44*, 89.
(20) Le Guillou, J. C.; Zinn-Justin, J. *Phys. Rev. B* **1980**, *21*, 3976−3998.
(21) Sano, M.; Kawaguchi, M.; Chen, Y. L.; Skarlupka, R. J.; Chang, T.; Zografi, G.; Yu, H. *Rev. Sci. Instrum.* **1986**, *57*, 1158.
(22) Lucassen-Reynders, E. H.; Lucassen, J. *J. Adv. Colloid Interface Sci.* **1969**, *2*, 347.
(23) Crilly, J. F.; Earnshaw, J. C. *Biophys. J.* **1983**, *41*, 197.
(24) Crilly, J. F.; Earnshaw, J. C. *Biophys. J.* **1983**, *41*, 211.
(25) Earnshaw, J. C.; McGivern, R. C.; McLaughlin, A. C.; Winch, P. J. *Langmuir* **1990**, *6*, 649.
(26) Esker, A. R. Molecular Architecture and Monolayer Dynamics at the Air/Water Interface by Surface Light Scattering. Ph.D. Thesis, University of Wisconsin−Madison, 1996.
(27) Kim, C.; Yu, H. *Langmuir* **2003**, *19*, 4460.
(28) Takahashi, A.; Yoshida, A.; Kawaguchi, M. *Macromolecules* **1982**, *15*, 1196.

MA0604643